Supporting Information

**Environmental Science and Technology**

# Abiotic Degradation of Chlorinated Solvents by Clay Minerals and Fe(II): Evidence for reactive mineral intermediates

*James Entwistle*[1], *Drew E. Latta*[2], *Michelle M. Scherer*[2], *and Anke Neumann*[1,*]

[1]School of Engineering, Newcastle University, Newcastle upon Tyne, NE 1 7RU, UK [2]Civil and Environmental Engineering, The University of Iowa, Iowa City, Iowa 52242, USA

* E-mail: anke.neumann@ncl.ac.uk

Pages: 17

Figures: 9

Tables: 6

## Analytical procedures

### Chlorinated compounds

GC-MS analysis of PCE, TCE, and DCE isomers was performed on an Agilent 7890A GC using split/split-less injection at 260 °C with Helium as the carrier gas (flow rate of 1 mL $min^{-1}$, initial pressure of 50 kPa, and split at 50 mL $min^{-1}$) and an Agilent 5975C MSD for mass detection. Compound separation was performed on a Restek fused silica capillary column (60 m × 0.25 mm i.d.) coated with 1.4 µm Rtx-VMS phase, applying a GC temperature program (initial temperature: 30 °C, hold for 8 minutes; ramp to 260 °C at 15 °C $min^{-1}$; hold at 260 °C for 6 minutes). The mass separation was performed using an Agilent 5975C MSD (electron voltage 70 eV, source temperature 230 °C), quad temperature 150 °C, multiplier voltage 1200 V, interface temperature 260 °C). The acquired data was processed using Chemstation, using an internal (CFB) and external standards. The measured concentrations were corrected for the extraction efficiency into n-pentane and for partitioning into the headspace, as detailed below.

### Gaseous products

Analysis of gaseous compounds (VC, acetylene, ethene, ethane) was performed on a Thermo Trace GC coupled to a flame ionization detector (FID). An Agilent CP-Silica Plot column (30 m × 0.32 mm i.d.) coated with a film 4 µm phase in conjunction with the GC temperature program (initial temperature: 75 °C, hold for 50 minutes; ramp to 225 °C at 15 °C $min^{-1}$; hold at 225 °C for 30 minutes) was used for compound separation. Target compounds were identified and quantified by comparing to a series of calibration curves which were created by injecting known volumes of gas standards (acetylene, 1% in $N_2$ balance, Calgaz; ethene, ethane, and VC, all 1% in $N_2$ balance, Calgaz). The total amounts of $C_2$ gases were calculated taking into account compound partitioning between aqueous and gas phase as well as the changing ratio of aqueous to gas phase due to aqueous phase sampling, as detailed below.

### Mössbauer spectroscopy

Samples for Mössbauer were analyzed using a MS4 Mössbauer spectrometer (SEE Co., Edina, MN, U.S.A.) in transmission mode and calibrated against 7 µm $\alpha$-Fe(0) foil. Temperature during spectra acquisition was controlled with a closed cycle cryostat (SHI-850, Janis Research Co., Wilmington, MA, U.S.A.) at either 13 K (reactors containing aqueous $^{56}$Fe(II)) or 77 K (reactors containing aqueous $^{57}$Fe(II)) to allow for quantifying the Fe speciation of the clay mineral and the aqueous Fe removed from solution, respectively. Mössbauer spectra were analyzed using the software Recoil and its Voigt-based fitting routine[4], which also provides the uncertainties of the fit parameters[3].

## Data evaluation

Responses from GC-MS analysis for PCE, TCE, and HCA were first normalized to the internal standard CFB and then converted into concentrations via linear regression of external standards. Concentrations were corrected for sample dilution (0.4 mL sample extracted into 0.6 mL n-pentane) and extraction efficiencies (Table S1), which were determined by comparing responses from standards prepared in n-pentane with those prepared in aqueous solution and subsequently extracted into n-pentane. Finally, total concentrations ($c_{i,tot}$) were calculated from the measured concentrations $c_{i,m}$, taking into account partitioning into the headspace of the reactors and changes in the volumes of headspace ($V_g$) and aqueous phase ($V_{aq}$) over the reaction time, which was due to repeated (x) removal of an aqueous sample of volume $V_{s,aq}$ (420 µL):

$$c_{i,tot} = \frac{K_{iH}(V_g + xV_{s,aq})c_{i,m} + (V_{aq} - xV_{s,aq})c_{i,m}}{V_{tot}} \tag{S1}$$

The compounds' dimensionless Henry's constants $K_{iH}$ were taken from a recent compilation[5] and are listed in Table S1, together with values for the parameters in equation S1.

Similarly, the amounts of gaseous products (acetylene, ethene, ethane) obtained from GC-FID ($n_{i,m}$) were converted into total amounts ($n_{i,tot}$), using the dimensionless Henry's constants $K_{iH}$ (Table S1), the volumes of headspace ($V_g$) and aqueous phase ($V_{aq}$), as well as sampling (x) of aqueous phase ($V_{s,aq}$ = 420 µL) and headspace ($V_{s,g}$ = 250 µL):

$$n_{i,tot} = \frac{n_{i,m}}{V_{s,g}}(V_g + xV_{s,aq}) + \frac{1}{K_{iH}}\frac{n_{i,m}}{V_{s,g}}(V_{aq} - xV_{s,aq}) \tag{S2}$$

**Table S1:** Parameters used to evaluate the total concentrations of PCE, TCE, and HCA as well as the total amounts of acetylene, ethene, and ethane in the reactors.

| parameter | PCE | TCE | HCA | actetylene | ethene | ethane |
|---|---|---|---|---|---|---|
| extraction efficiency | 93.8% | 80.7 % | 94.5 % | n.a.[b] | n.a.[b] | n.a.[b] |
| $K_{iH}$[a] | 1.186 | 0.367 | 0.098 | 0.984 | 8.583 | 21.23 |
| $V_a$ | 5 mL | 5 mL | 5 mL | 5 mL | 5 mL | 5 mL |
| $V_w$ | 155 mL | 155 mL | 20 mL | 155 mL | 155 mL | 155 mL |
| $V_{tot}$ | 160 mL | 160 mL | 25 mL | 160 mL | 160 mL | 160 mL |

[a] Dimensionless Henry's constant, $K_{iH} = \frac{c_{i,g}}{c_{i,aq}}$, values taken from a recent compilation[5].
[b] n.a.: not applicable.

## Figures and Tables

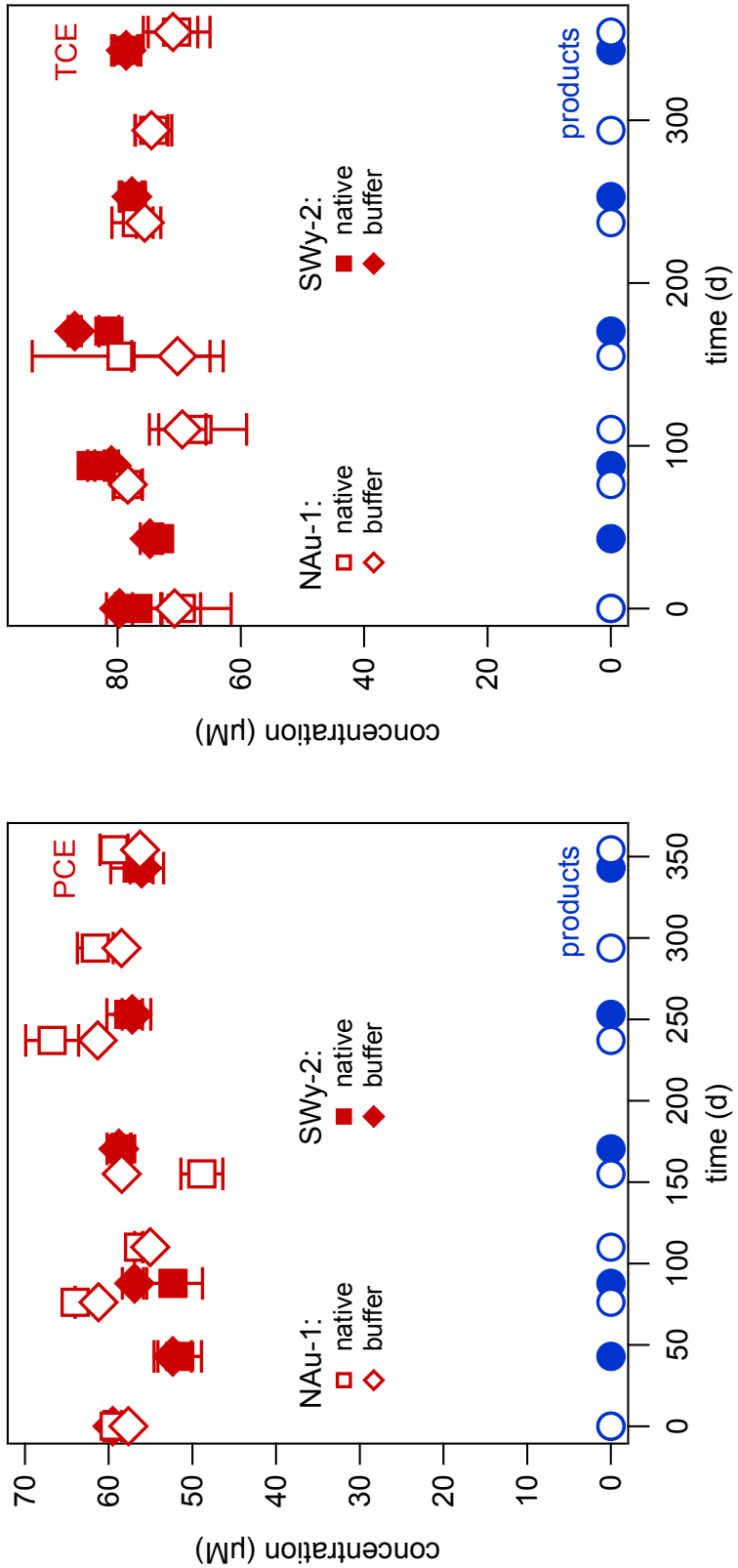


**Figure S1:** PCE and TCE concentrations in reference reactors containing buffer only to control for reactant loss due to volatilization or clay minerals NAu-1 or SWy-2 in their native form (buffered to pH 8) to quantify sorption to the mineral surfaces. No dechlorination products were detected in any of these reactors. Error bars represent the standard deviation of duplicate reactors.

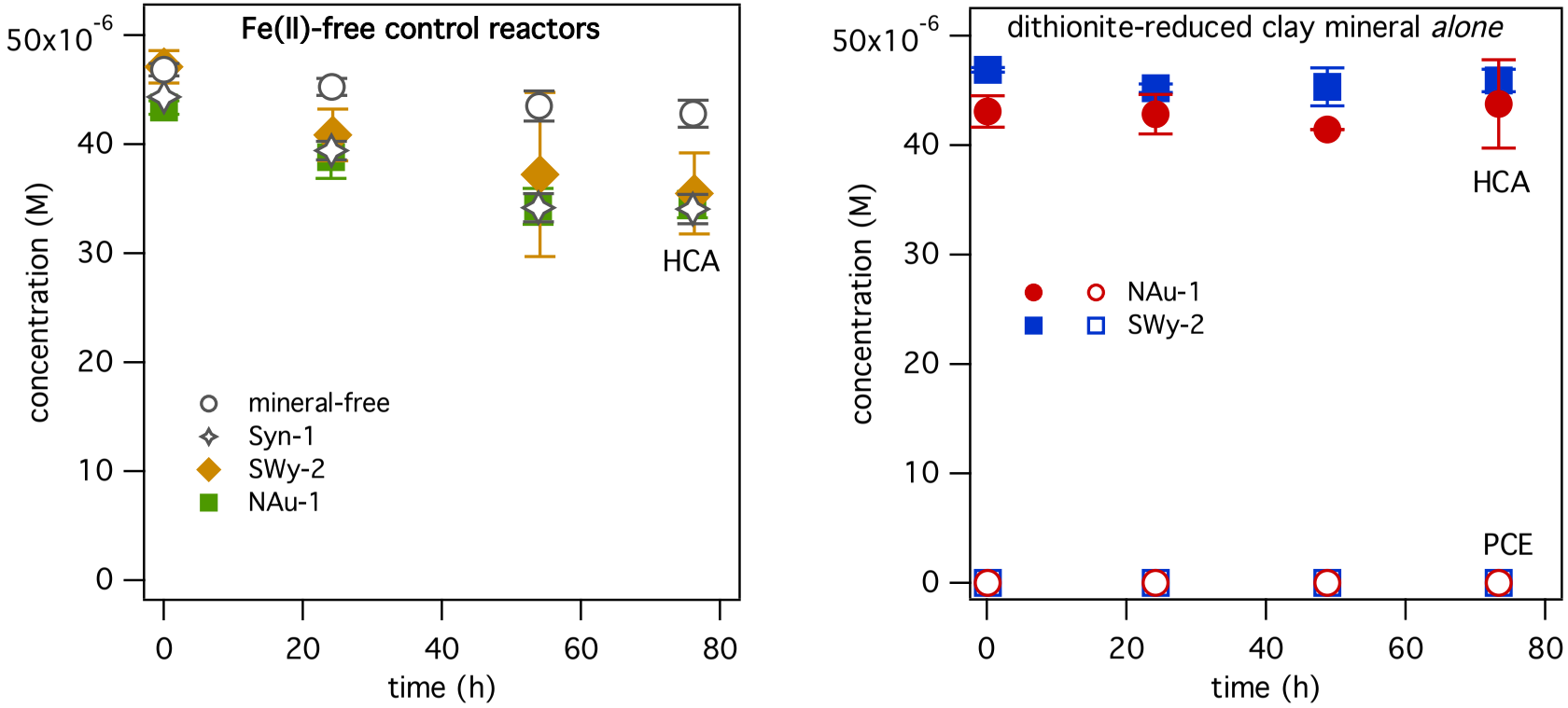


**Figure S2:** HCA concentrations measured in reference reactors containing no added aqueous Fe(II) (left) and in the presence of dithionite-reduced clay minerals (right). Left: Mineral-free reactors (grey open circles) monitored any losses of HCA due to volatilization (limited: 8.6±0.1%) and native mineral reactors monitored losses of HCA due to sorption (small: 17±0.5%). There is no statistically significant difference between Fe-free clay mineral Syn-1 (grey open stars) and Fe-bearing clay minerals SWy-2 and NAu-1 (filled orange diamonds and green squares, respectively). Right: Similar to PCE and TCE, HCA was not degraded by structural Fe(II) in clay minerals *alone* over the time frame of the experiments (80 hours). We note that loss due to volatilization and sorption was smaller in experiments with dithionite-reduced NAu-1 (red circles) and SWy-2 (blue squares) compared to the native clay minerals. Error bars represent standard deviations from replicate experiments.

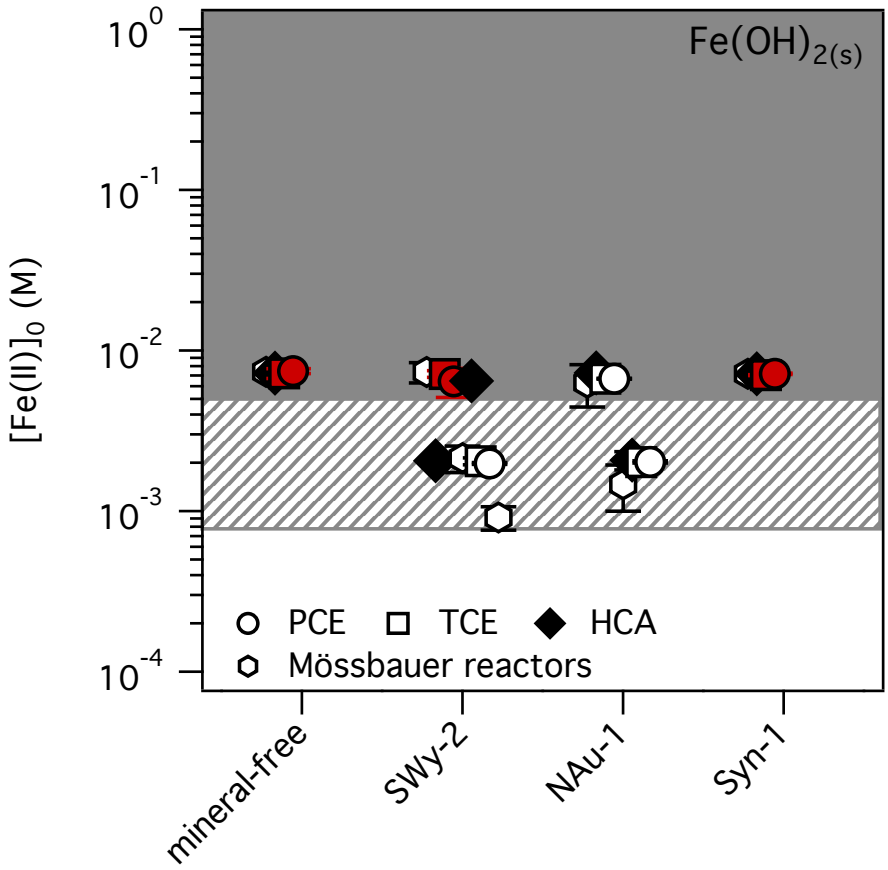


**Figure S3:** Initial Fe(II) activities in PCE, TCE, HCA, and Mössbauer reactors containing clay minerals and mineral-free suspension, overlaid with the solubility of $Fe(OH)_2$. Filled markers represent reactors in which dechlorination products were detected and open black markers are reactors without product formation. The grey hatched and shaded areas represent the Fe(II) concentrations expected to lead to $Fe(OH)_2$ precipitation and were calculated based on the range of published solubility product values ($-15.11 < \log K_{sp}(Fe(OH)_2) < -14.30$)[1,2,6] . Measured Fe(II) concentrations were converted into activities based on the ionic strength in the reactors (details in Table S6).

**Figure S4:** Reactors of differently prepared high Fe content clay mineral NAu-1: native, amended with aqueous Fe(II) at concentrations of 4.4 mM or 20.5 mM, and dithionite-reduced (from left to right).

**Figure S5:** Reactors of differently prepared low Fe content clay mineral SWy-2: native, amended with aqueous Fe(II) at concentrations of 1.9 mM, 4.9 mM, or 20.1 mM, and dithionite-reduced (from left to right).

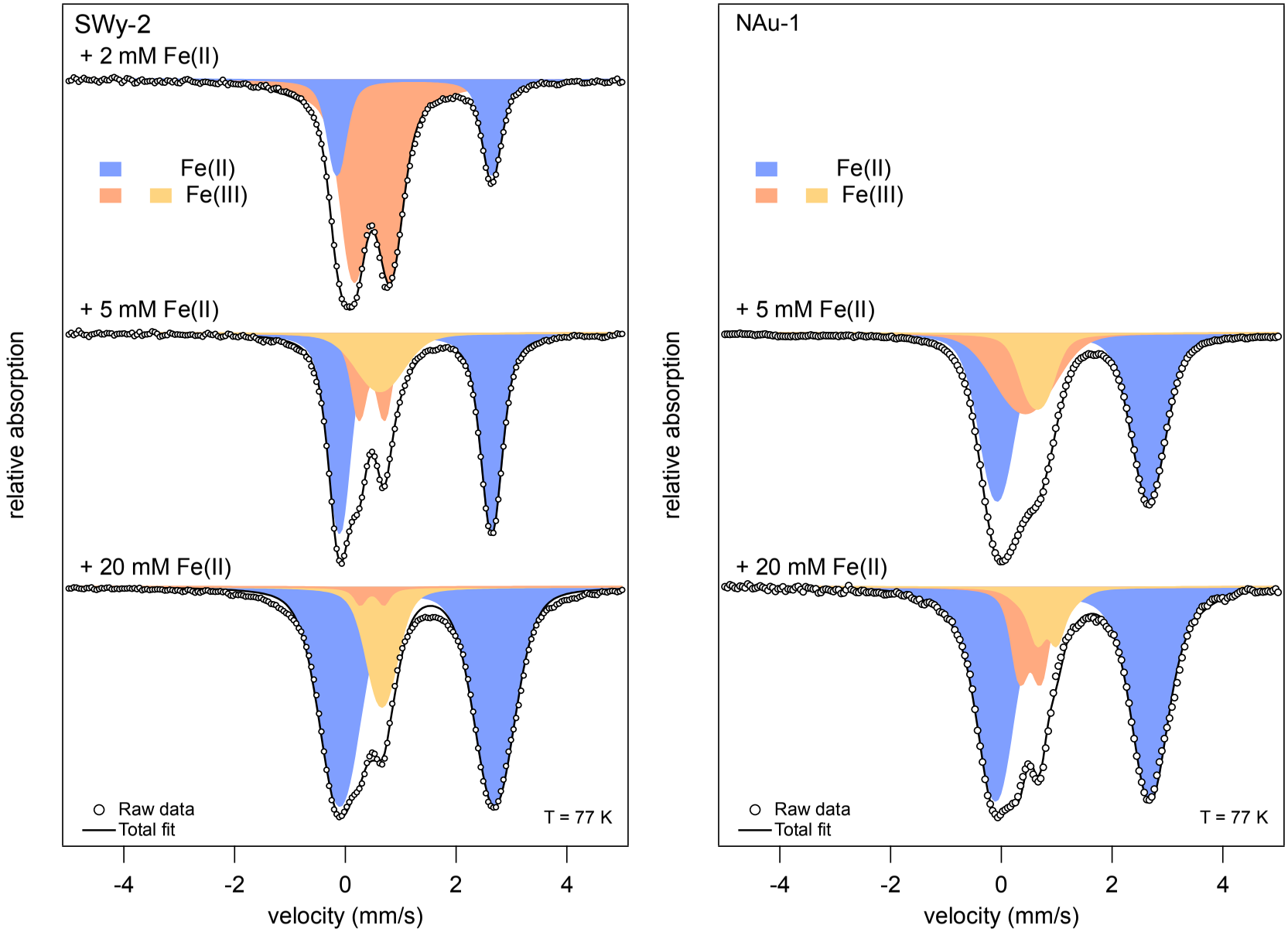


**Figure S6:** Mössbauer spectra of low Fe content clay mineral SWy-2 (left) and high Fe content clay mineral NAu-1 (right) after reaction with different concentrations of Mössbauer-visible $^{57}$Fe(II). The signal associated with $^{57}$Fe in both clay minerals comprises $\leq$3.2% of the total spectral area and the spectra thus reflect exclusively the Fe speciation of Fe(II) added and taken up from solution. The presence of both blue and yellow doublets indicates that all precipitates contain Fe(II) and Fe(III), respectively, and the ratio of Fe(II)/Fe(total) increased with increasing aqueous Fe(II) concentration from 25% to 80% for SWy-2 and from 62% to 75% for NAu-1 (Table S4). Spectra were collected at 77 K.

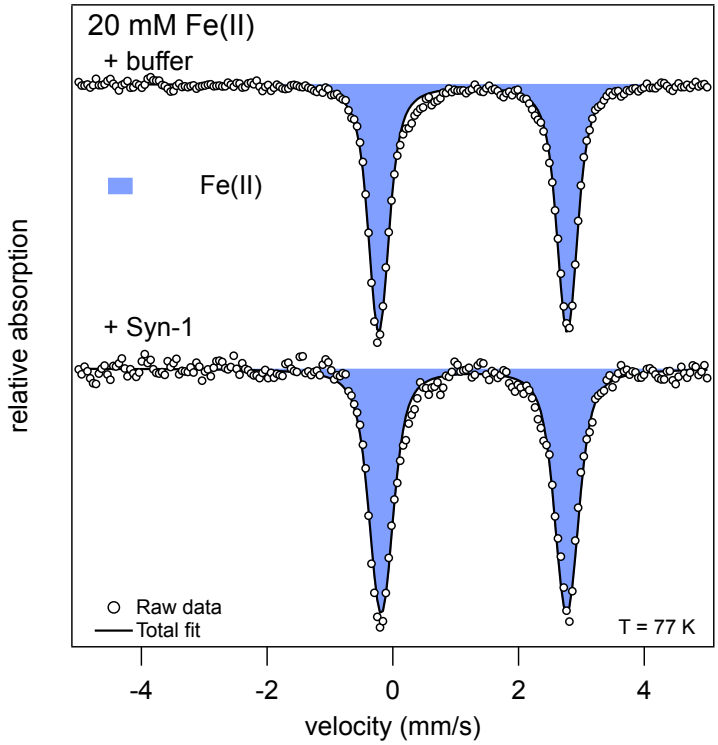


**Figure S7:** Mössbauer spectra of the precipitates formed in 20 mM $^{57}$Fe(II) solution in the absence of clay mineral (top) and in the presence of Fe-free clay mineral Syn-1 (bottom) show the presence of exclusively Fe(II) (blue doublet), indicating the absence of electron transfer and accidental oxidation. Spectra were collected at 77 K.

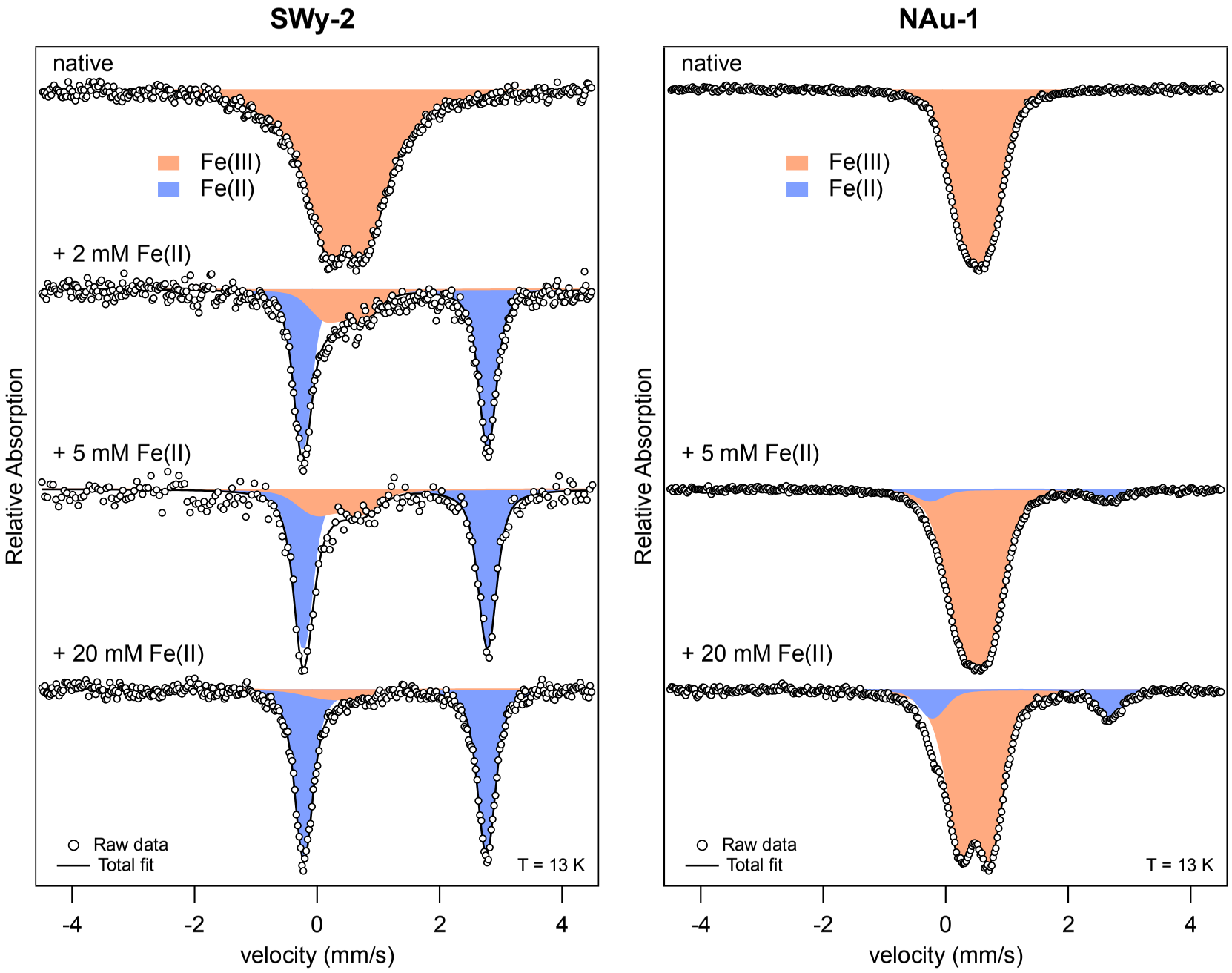


**Figure S8:** Mössbauer spectra of low Fe content clay mineral SWy-2 (left) and high Fe content clay mineral NAu-1 (right) before and after reaction with different concentrations of Mössbauer-invisible $^{56}$Fe(II). While both native clay minerals only contain Fe(III), as indicated by the presence of the yellow doublet, reaction with $^{56}$Fe(II) led to the formation of Fe(II) in the clay mineral structure (blue doublets). Clay mineral Fe reduction extents achieved were 78-93% for SWy-2 and 7-15% for NAu-1 (Table S4). Spectra were collected at 13 K.

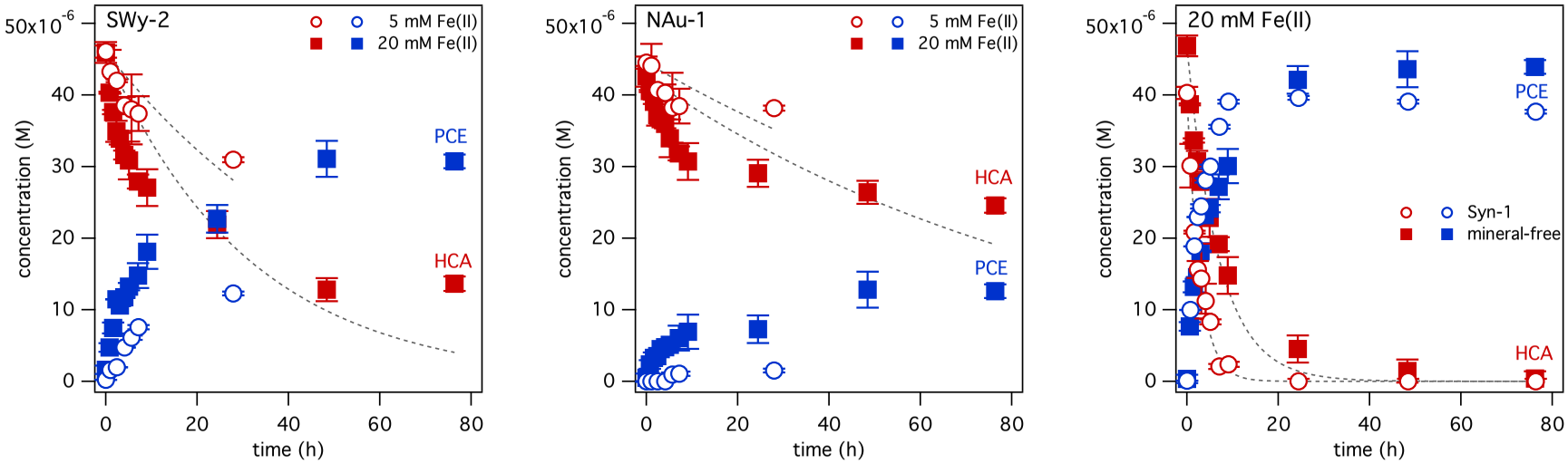


**Figure S9:** Kinetic data of the transformation of hexachloroethane (HCA, red) to PCE (blue) in suspensions of SWy-2 and NAu-1 reacted with 5 mM Fe(II) (open circles) and 20 mM Fe(II) (filled squares) as well as in 20 mM Fe(II) solution without the addition of clay mineral (filled squares) and in the presence of Fe-free Syn-1 (open circles). Dashed lines are fits to the first-order kinetic model (equation **??**), which does not describe the data well. Error bars represent the standard deviation of duplicate reactors.

**Table S2:** Summary of reactor conditions for PCE and TCE degradation experiments, including reactant loss and product formation observed. Errors are standard deviations from replicate reactors.

| Clay mineral | reactor condition | clay mineral Fe(II)/Fe(total)[a] | clay mineral concentration | initial reactant concentration | | reactant loss[b] | | product formation[c] | |
|---|---|---|---|---|---|---|---|---|---|
| | | % | $g\ L^{-1}$ | $\mu M$ | | % | | % | |
| | | | | PCE | TCE | PCE | TCE | PCE | TCE |
| NAu-1 | 5 mM Fe(II) | 6.9(0.6) | 5 | 53.8(1.9) | 73.3(9.0) | 5.6(0.3) | -2.0(0.4) | 0 | 0 |
| | 20 mM Fe(II) | 15.4(0.7) | 5 | 50.4(1.3) | 69.9(3.3) | 4.2(0.2) | -2.3(0.2) | 0 | 0 |
| | Dithionite-reduced | 90.1(0.3) | 3.5 | 50.8(1.4) | 68.7(1.8) | 4.9(0.3) | -1.1(0.1) | 0 | 0 |
| | Native | n.d.[e] | 5 | 59.3(0.1) | 69.7(3.1) | -0.1(0.0) | -1.1(0.1) | 0 | 0 |
| | Buffer | – | – | 57.6 | 70.7(9.2) | 2.4 | -0.4(0.1) | 0 | 0 |
| SWy-2 | 5 mM Fe(II) | 79.4(3.8) | 5 | 64.0(0.3) | 71.7(2.9) | 5.2(0.1) | -2.1(0.1) | 0 | 0 |
| | 20 mM Fe(II) | 92.5(1.9) | 5 | 55.4(7.0) | 73.0(4.6) | 3.7(0.5) | 4.3(0.3) | 17.4(1.3) | 15.0[d] |
| | Dithionite-reduced | 80.9[f] | 4.15 | 55.0(5.9) | 75.1(2.9) | -1.0(0.2) | -3.8(0.3) | 0 | 0 |
| | Native | n.d.[e] | 5 | 58.8(1.5) | 76.7(3.7) | 3.7(0.2) | -2.5(0.2) | 0 | 0 |
| | Buffer | – | – | 59.5(1.1) | 79.7(2.1) | 5.8(0.2) | 1.4(0.1) | 0 | 0 |
| Syn-1 | 20 mM Fe(II) | – | | 62.5(0.5) | 82.5(8.5) | 15(4) | 28(12) | 23.1(0.3) | 23.6(0.4) |
| – | 20 mM Fe(II) | – | – | 65.0(1.2) | 80.6(5.1) | 8.4(0.5) | 8.4(0.6) | 20.9(0.4) | 19.9(1.7) |

[a] Reduction extent of the clay mineral Fe as measured by HF digestion or Mössbauer spectroscopy (latter data from Table S4).
[b] Relative to the initial reactant concentration. [c] Refers to the sum of products formed in reactors containing either PCE or TCE as a starting reactant; relative to the initial reactant concentration. [d] Only one replicate reactor yielded products. [e] Not detected using Mössbauer spectroscopy.
[f] Only one replicate sample was subjected to the HF digestion and subsequent 1,10-phenanthroline analysis.

**Table S3:** Distribution of products formed in reactors containing 20 mM aqueous Fe(II) and different (clay) minerals. Errors are standard deviations from replicate reactors.

| **Reactor condition** | **PCE transformation** | | | | | **TCE transformation** | | | | |
|---|---|---|---|---|---|---|---|---|---|---|
| | products | ethane | ethene | acetylene | $[Fe(II)_r]$[a] | products | ethane | ethene | acetylene | $[Fe(II)_r]$[a] |
| | % of initial | % of overall products | | | M | % of initial | % of overall products | | | M |
| SWy-2 | 17.4(1.3) | 13.6(1.0) | 27.3(3.6) | 59.1(7.3) | $6.84\times10^{-5}$ | 15.0[b] | 6.8[b] | 22.9[b] | 70.2[b] | $3.77\times10^{-5}$ |
| Syn-1 | 23.1(0.3) | 10.1(0.2) | 20.3(1.2) | 69.7(1.4) | $9.84\times10^{-5}$ | 23.6(0.4) | 7.8(0.2) | 20.3(1.2) | 71.9(2.0) | $5.90\times10^{-5}$ |
| mineral-free | 20.9(0.4) | 10.9(0.2) | 22.8(1.2) | 66.4(2.0) | $9.02\times10^{-5}$ | 19.9(1.7) | 9.9(0.9) | 27.4(2.7) | 62.7(10.1) | $5.23\times10^{-5}$ |

[a] Calculated from the initial concentration of PCE or TCE, the amounts of products formed, and the stoichiometric factor $\nu$ accounting for the transfer of 10(8), 8(6), or 6(4) electrons from reactive Fe(II) for the formation of ethane, ethene, or acetylene from PCE(TCE), respectively.

[b] Only one replicate reactor yielded products.

**Table S4:** Mössbauer hyperfine parameters from clay minerals reacted with aqueous $^{56}$Fe(II) to determine structural Fe reduction extent and reacted with $^{57}$Fe(II) to determine the Fe speciation of the precipitates formed. Spectra were acquired at 13 K and 77 K, respectively. Voigt-based fitting was used to evaluate the Mössbauer parameters[4] .

| | $\chi^2$ | Site | CS[a] *mm/s* | QS ($\sigma$)[b] *mm/s* | area ($\sigma$)[c] *%* |
|---|---|---|---|---|---|
| **$^{56}$Fe(II)-reacted clay minerals** | | | | | |
| **SWy-2** | | | | | |
| **native** | 0.64 | Fe(III) | 0.48 | 10.9(0.92) | 100 |
| **+2 mM Fe(II)** | 0.54 | Fe(II) | 1.27 | 3.02(0.17) | 77.8(2.0) |
| | | Fe(III) | 0.43 | 0.61(0.39) | 22.2(2.0) |
| **+5 mM Fe(II)** | 0.55 | Fe(II) | 1.28 | 3.01(0.19) | 79.4(3.8) |
| | | Fe(III) | 0.34 | 0.76(0.45) | 20.6(3.8) |
| **+20 mM Fe(II)** | 0.57 | Fe(II) | 1.27 | 2.98(0.18) | 92.5(1.9) |
| | | Fe(III) | 0.32 | 0.64(0.47) | 7.5(1.9) |
| **NAu-1** | | | | | |
| **native** | 0.58 | Fe(III) | 0.50 | 0.50(0.34) | 100 |
| **+5 mM Fe(II)** | 0.62 | Fe(II) | 1.20 | 2.91(0.33) | 6.9(0.6) |
| | | Fe(III) | 0.49 | 0.53(0.35) | 93.1(0.6) |
| **+20 mM Fe(II)** | 0.69 | Fe(II) | 1.23 | 2.89(0.30) | 15.4(0.7) |
| | | Fe(III) | 0.49 | 0.55(0.34) | 84.6(0.7) |
| **$^{57}$Fe(II)-reacted clay minerals** | | | | | |
| **SWy-2** | | | | | |
| **+2 mM Fe(II)** | 1.50 | Fe(II) | 1.25 | 2.80(0.22) | 25.4(0.3) |
| | | Fe(III) | 0.48 | 0.96(0.93) | 74.6(0.3) |
| **+5 mM Fe(II)** | 1.26 | Fe(II) | 1.27 | 2.75(0.26) | 62.6(0.2) |
| | | Fe(III) 1 | 0.47 | 0.46(0.13) | 19.4(0.2) |
| | | Fe(III) 2 | 0.62 | 0.60(0.45) | 18.0(0.2) |
| **+20 mM Fe(II)** | 12.46 | Fe(II) | 1.30 | 2.79(0.62) | 80.3(0.5) |
| | | Fe(III) 1 | 0.48 | 0.43(0) | 2.4(0.4) |
| | | Fe(III) 2 | 0.66 | 0.34(0.25) | 17.3(0.4) |
| **NAu-1** | | | | | |
| **+5 mM Fe(II)** | 6.31 | Fe(II) | 1.29 | 2.74(0.51) | 62.3(0.3) |
| | | Fe(III) 1 | 0.43 | 0.76(0.56) | 24.4(0.3) |
| | | Fe(III) 2 | 0.65 | 0.35(0.24) | 13.3(0.2) |
| **+20 mM Fe(II)** | 2.19 | Fe(II) | 1.29 | 2.85(0.79) | 75.2(0.1) |
| | | Fe(III) 1 | 0.50 | 0.39(0.01) | 11.9(0.1) |
| | | Fe(III) 2 | 0.70 | 0.29(0.01) | 11.2(0.1) |
| **Syn-1** | | | | | |
| **+20 mM Fe(II)** | 0.72 | Fe(II) | 1.29 | 2.95(0.26) | 100 |
| **mineral-free** | | | | | |
| **+20 mM Fe(II)** | 0.97 | Fe(II) | 1.27 | 3.00(0.20) | 100 |

[a] Center shift relative to $\alpha$-Fe(0).
[b] Standard deviation of QS from the Gaussian distribution of the QS parameter used in the model. [c] Standard deviation due to uncertainty.

**Table S5:** Data from reduction capacity experiments using HCA, at initial Fe(II) concentrations of ∼20 mM. From both decrease in HCA concentration and increase in PCE concentration, maximum reactive Fe(II) concentration and its proportion of the total Fe(II) in the reactors were calculated. Experiments were run for 750 hours.

| **Reactor** | **HCA** | | | | **PCE** | | |
|---|---|---|---|---|---|---|---|
| | initial | final | reactive Fe(II)[a] | reactive Fe(II)/total Fe(II)[b] | final | reactive Fe(II)[c] | reactive Fe(II)/total Fe(II)[b] |
| | *mM* | *mM* | *mM* | % | *mM* | *mM* | % |
| Syn-1 | 1.33(0.01) | 1.16(0.01) | 0.34(0.01) | 1.62 | 0.22(0.00) | 0.44(0.01) | 2.12 |
| mineral-free | 1.02(0.02) | 0.85(0.01) | 0.33(0.02) | 1.54 | 0.28(0.00) | 0.56(0.01) | 2.65 |

[a] Reactive Fe(II) was calculated as the difference of initial and final HCA concentration and taking into account the stoichiometry of the reduction of HCA to PCE requiring the oxidation of two Fe(II): $[\mathrm{Fe(II)}_{\mathrm{reactive}}] = 2 \times \left([\mathrm{HCA}]_{\mathrm{initial}} - [\mathrm{HCA}]_{\mathrm{final}}\right)$

[b] Total Fe(II) was taken from Table **??**. For reactors containing Syn-1: 20.9 mM, for mineral-free reactors: 21.1 mM.

[c] Reactive Fe(II) was calculated taking into account the stoichiometry of the reduction of HCA to PCE requiring the oxidation of two Fe(II): $[\mathrm{Fe(II)}_{\mathrm{reactive}}] = 2 \times [\mathrm{PCE}]_{\mathrm{final}}$.

**Table S6:** Overview of Fe(II) concentrations in the experimental reactors and conversion calculation into activities for comparison to the solubility product of $Fe(OH)_2$ (Figure S3).

| Reactor | 2 mM | | | | 5 mM | | | | 20 mM | | | |
|---|---|---|---|---|---|---|---|---|---|---|---|---|
| | initial concentration[a] *mM* | ionic strength[b] *M* | activity coefficient[c] | activity *mM* | initial concentration[a] *mM* | ionic strength[b] *M* | activity coefficient[c] | activity *mM* | initial concentration[a] *mM* | ionic strength[b] *M* | activity coefficient[d] | activity *mM* |
| **PCE** | | | | | | | | | | | | |
| mineral-free | | | | | | | | | 21.9(0.6) | 0.121 | 0.34 | 7.45(0.27) |
| SWy-2 | | | | | 5.21(0.05) | 0.071 | 0.38 | 1.98(0.03) | 18.3(2.7) | 0.110 | 0.35 | 6.44(1.32) |
| NAu-1 | | | | | 5.34(0.05) | 0.071 | 0.38 | 2.03(0.03) | 19.1(0.1) | 0.112 | 0.35 | 6.68(0.05) |
| Syn-1 | | | | | | | | | 20.9(0.1) | 0.118 | 0.34 | 7.18(0.06) |
| **TCE** | | | | | | | | | | | | |
| mineral-free | | | | | | | | | 21.0(1.0) | 0.118 | 0.34 | 7.22(0.50) |
| SWy-2 | | | | | 5.41(0.19) | 0.071 | 0.38 | 2.05(0.10) | 20.8(0.7) | 0.117 | 0.34 | 7.15(0.34) |
| NAu-1 | | | | | 5.31(0.04) | 0.071 | 0.38 | 2.02(0.02) | 19.1(0.4) | 0.112 | 0.35 | 6.68(0.18) |
| Syn-1 | | | | | | | | | 20.4(0.08) | 0.116 | 0.35 | 7.04(0.04) |
| **HCA** | | | | | | | | | | | | |
| mineral-free | | | | | | | | | 21.1(0.2) | 0.118 | 0.34 | 7.24(0.11) |
| SWy-2 | | | | | 5.08(0.02) | 0.070 | 0.38 | 1.94(0.01) | 21.1(0.1) | 0.118 | 0.34 | 7.23(0.04) |
| NAu-1 | | | | | 5.50(0.51) | 0.071 | 0.38 | 2.08(0.27) | 21.2(0.47) | 0.119 | 0.34 | 7.26(0.23) |
| Syn-1 | | | | | | | | | 20.9(0.3) | 0.118 | 0.34 | 7.17(0.14) |
| **Mössbauer[e]** | | | | | | | | | | | | |
| mineral-free[f] | | | | | | | | | 21.6 | 0.120 | 0.34 | 7.38 |
| SWy-2 | 2.28(0.27) | 0.062 | 0.40 | 0.91(0.15) | 5.67(0.75) | 0.072 | 0.38 | 2.14(0.40) | 21.5(2.2) | 0.119 | 0.34 | 7.35(1.07) |
| NAu-1 | | | | | 3.79(0.85) | 0.066 | 0.39 | 1.47(0.47) | 17.9(3.7) | 0.109 | 0.35 | 6.30(1.86) |
| Syn-1[f] | | | | | | | | | 20.9 | 0.118 | 0.34 | 7.18 |

[a] Average values from duplicate experiments. Aqueous Fe(II) concentrations were measured using the 1,10-phenanthroline method[7]. [b] The ionic strength $I$ was calculated from the measured concentrations $c_i$ and the the charge of the ions, $z_i$: $I = \frac{1}{2}\sum c_i z_i^2$ [8]. Ions present in solution were: Fe(II), $Cl^-$ (2x the concentration of Fe(II)), $Na^+$ and $Cl^-$ (0.05 M), and MOPS anion (0.01 M). [c] The activity coefficient $f$ was calculated using the Güntelberg approximation: $\log f = -0.5z^2 \frac{\sqrt{I}}{1+\sqrt{I}}$ [8]. [d] The activity coefficient $f$ was calculated using the Davies approximation: $\log f = -0.5z^2\left(\frac{\sqrt{I}}{1+\sqrt{I}} - 0.2I\right)$ [8]. [e] Average values from experiments with $^{56}Fe(II)$ and $^{57}Fe(II)$. [f] Only one reactor was prepared for Mössbauer analysis.

# References


[1] G. Bohnsack. Löslichkeit und thermodynamische daten von eisen(ii)-hydroxid durch analytische bestimmung des eisens und leitfähigkeitsmessung im system eisen-wasser. *Berichte der Bunsengesellschaft für physikalische Chemie*, 92(7):797–802, 1988.

[2] J. P. Gustafsson. Visual minteq, 3.0, 2011.

[3] K. Lagarec and D.G. Rancourt. Recoil - mössbauer spectral analysis software for windows, 1998.

[4] D. G. Rancourt and J. Y. Ping. Voigt-based method for arbritrary-shape static hyperfine parameter distributions on mössbauer-spectroscopy. *Nucl Instrum Methods Phys Res B*, 58(1):85–97, 1991.

[5] R. Sander. Compilation of Henry's law constants (version 4.0) for water as solvent. *Atmospheric Chemistry and Physics*, 15(8):4399–4981, 2015.

[6] C. N. Sawyer, P. L. McCarty, and G. F. Parkin. *Chemistry for environmental engineering and science*. 2016.

[7] Alfred A Schilt. *Analytical applications of 1, 10-phenanthroline and related compounds: international series of monographs in analytical chemistry*. Pergamon Press, 1969.

[8] W. Stumm and J. J. Morgan. *Aquatic Chemistry: Chemical Equilibria and Rates in Natural Waters*. Wiley, New York, 1996.